



HAL
open science

Color fundus image enhancement - A deep learning based desktop app for earlier screening of diabetic retinopathy using real-time handheld fundus camera

El-Mehdi Chakour, Zineb Sadok, Mohamed Akil, Rostom Kachouri, Anas Mansouri, Idriss Benatiya, Ali Ahaitouf

► To cite this version:

El-Mehdi Chakour, Zineb Sadok, Mohamed Akil, Rostom Kachouri, Anas Mansouri, et al.. Color fundus image enhancement - A deep learning based desktop app for earlier screening of diabetic retinopathy using real-time handheld fundus camera. International Conference on Optimization and Data Science in Industrial Engineering (ODSIE 2023), Nov 2023, Istanbul, Turkey. hal-04451313

HAL Id: hal-04451313

<https://hal.science/hal-04451313>

Submitted on 11 Feb 2024

HAL is a multi-disciplinary open access archive for the deposit and dissemination of scientific research documents, whether they are published or not. The documents may come from teaching and research institutions in France or abroad, or from public or private research centers.

L'archive ouverte pluridisciplinaire **HAL**, est destinée au dépôt et à la diffusion de documents scientifiques de niveau recherche, publiés ou non, émanant des établissements d'enseignement et de recherche français ou étrangers, des laboratoires publics ou privés.

COLOR FUNDUS IMAGE ENHANCEMENT – A DEEP LEARNING BASED DESKTOP APP FOR EARLIER SCREENING OF DIABETIC RETINOPATHY USING REAL-TIME HANDHELD FUNDUS CAMERA

El-Mehdi Chakour
Laboratory of Intelligent Systems,
Geo-resources and Renewable
Energies, Faculty of Sciences and
Technology, Sidi Mohamed Ben
Abdellah University, Fez, Morocco.
elmehdi.chakour@usmba.ac.ma

Zineb Sadok
Laboratory of Intelligent Systems,
Geo-resources and Renewable
Energies, Faculty of Sciences and
Technology, Sidi Mohamed Ben
Abdellah University, Fez, Morocco.
zineb.sadok@usmba.ac.ma

Mohamed Akil
Gaspard Monge Computer Science
Laboratory, ESIEE Paris
Gustave Eiffel University
F-77454 Marne-la-Vallée, France.
mohamed.akil@esiee.fr

Rostom Kachouri
Gaspard Monge Computer Science
Laboratory, ESIEE Paris
Gustave Eiffel University
F-77454 Marne-la-Vallée, France.
rostom.kachouri@esiee.fr

Anas Mansouri
Laboratory of Intelligent Systems,
Geo-resources and Renewable
Energies, Faculty of Sciences and
Technology, Sidi Mohamed Ben
Abdellah University, Fez, Morocco.
anas.mansouri@usmba.ac.ma

Ali Ahaitouf
Laboratory of Intelligent Systems,
Geo-resources and Renewable
Energies, Faculty of Sciences and
Technology, Sidi Mohamed Ben
Abdellah University, Fez, Morocco.
ali.ahaitouf@usmba.ac.ma

Idriss Benatiya Andaloussi
Ophtalmology Department Hassan II
Hospital, Sidi Mohammed Ben Abdellah
University, Fez, Morocco.
idriss.benatiyaandaloussi@usmba.ac.ma

Abstract— Diabetic retinopathy (DR) is a common complication of diabetes that affects the blood vessels in the retina. It is a leading cause of vision loss worldwide. Early detection and intervention are crucial in preventing irreversible damage to the eyes. In this study, we propose a computer-aided diagnosis (CAD) system for the early detection of DR. Using a portable non-mydratic fundus camera, we captured retinal images and applied deblurring and contrast enhancement techniques to improve image quality. We employed fine-tuning and transfer learning, specifically utilizing DenseNet-121, to detect DR from our private dataset. Additionally, two large datasets, APTOS and EyePACS, were used to train and evaluate different transfer learning DNN models. We found that the DenseNet-121 network achieves better results of accuracy with 97.3856 and 90.9000 respectively for APTOS and EyePACS datasets. The denseNet-121 is also used to detect DR from our private dataset and gives a higher accuracy of 98.6111. This work has designed a deep learning-based Desktop app, which captures and processes the fundus images for earlier screening of DR in remote medical centers or areas with limited access to Table-top fundus cameras and ophthalmologists.

Keywords— A deep learning based Desktop app, earlier screening of DR, real-time eye diagnosis, handheld fundus camera.

I. INTRODUCTION

According to the WHO (World Health Organization), at least 2.2 billion people worldwide suffer from visual impairment. Age-related macular degeneration, cataracts, diabetic retinopathy, and glaucoma are some of the main reasons. The International Diabetes Federation (IDF) estimated that in 2019 there were 463 million diabetics worldwide, and that number is expected to rise to 700 million by 2025. Diabetic

Retinopathy is a complication, considered to be a consequence of diabetes [1].

The top three regions where diabetic retinopathy (DR) prevalence is reported to be the highest are: Africa (35.9%, i.e., 6.99 million), Middle East and North Africa (32.9%, i.e., 18.07 million) and North America and Caribbean (33.3%, i.e., 15.89 million). DR is one of the main causes of blindness and visual impairment in adults aged 50 and over. The higher rate of untreated eye diseases in low-income areas further exacerbates the DR related problem. Additionally, with population growth and the aging of the population, the risk of more people suffering from such visual impairment also increases.

It is therefore essential to conduct screening, that will help in early diagnosis of DR, which is easier during the initial stage of the condition called Non-Proliferative Diabetic Retinopathy. However, this screening often requires expensive equipment which is available only in ophthalmology centers. Moreover, scheduling routine preventative checkups with an ophthalmologist are challenging in rural locations, further hindering the early identification of DR. Therefore, the screening needs to be accessible, calling for an automated system Computer Aided Diagnosis (CAD), which is mobile, has low cost and is easy to use by oculist, orthoptist, nurse.

Such a system must ensure the acquisition of patient fundus images in "real time" using portable retinal cameras (non-mydratic fundus camera) connected either to Desktops or smartphones, which will provide the screening results, thereby assisting in early diagnosis of DR. Once the diagnosis results are established during the consultation, in-depth

examination by ophthalmologists takes place at a remote ophthalmology site [2].

The research presented in this article is part of a project that aims to designing and developing an automatic system to assist in early detection and diagnosis of ocular pathologies, using fundus images of the eye captured by portable retinal cameras. The target system - once ready - could be deployed on pilot sites as part of tele-ophthalmology networks. One such deployment is aimed towards the Fez region of Morocco, with a current diabetic patient count of 1.5 million and is expected to increase to 2.6 million by 2030 [Reference: Ipos Health Care]. As per Moroccan Society of Ophthalmology, the main cause of blindness is DR, affecting 50% of type 2 diabetes patients. However, lesions that can be detected on fundus imaging are caused by the early stages of DR. Early detection enables the provision of preventative treatment with the objective of halting DR development, thereby reducing the risks of irreparable eye damage.

Our target system developed as a tele-ophthalmology-based application (Fig.1), will constitute a novel approach of providing itinerant visual care in rural areas of Fez and its region (Rural Eye Care), connected to a pilot site at the Tertiary Ophthalmology Center and Vision Center at Omar Drissi Hospital, CHU HASAN II, Fez. This will eventually help to overcome the serious dearth of ophthalmologists. There are currently only 330 ophthalmologists, working in the public sector, whereas more than 80 % of the private sector's ophthalmologists are centered on the Casablanca-Kenitra axis [3].

artefacts, making them both challenging to interpret (analyzable on observation by ophthalmologists) and potentially degrading the robustness of the automatic system for early detection and diagnosis of DR.

This work has the following contributions:

1. We conduct a comprehensive and comparative study of techniques for enhancing fundus images captured by portable retinal cameras. We evaluate each of these noise reduction and contrast enhancement techniques, using the image quality evaluation metrics (PNSR, SSIM, RCEF). This evaluation enabled us to build different improvement chains, comparatively evaluate them, and then exploit the most relevant one in the pre-treatment step-upstream of the automatic system of aid in early detection of DR. This study has resulted in a software framework ensures the acquisition of quality and interpretable images.
2. Our proposed CAD system relies on a Fine-Tuning model of deep transfer learning-based models for DR detection. A private image database of patients from the ophthalmology department of the Omar Drissi Hospital, CHU HASAN II, Fez, as well as public fundus image databases such as APTOS and EyePACS are used. We evaluate our system using several metrics such as accuracy, precision, sensitivity, specificity and, F1-score. The images

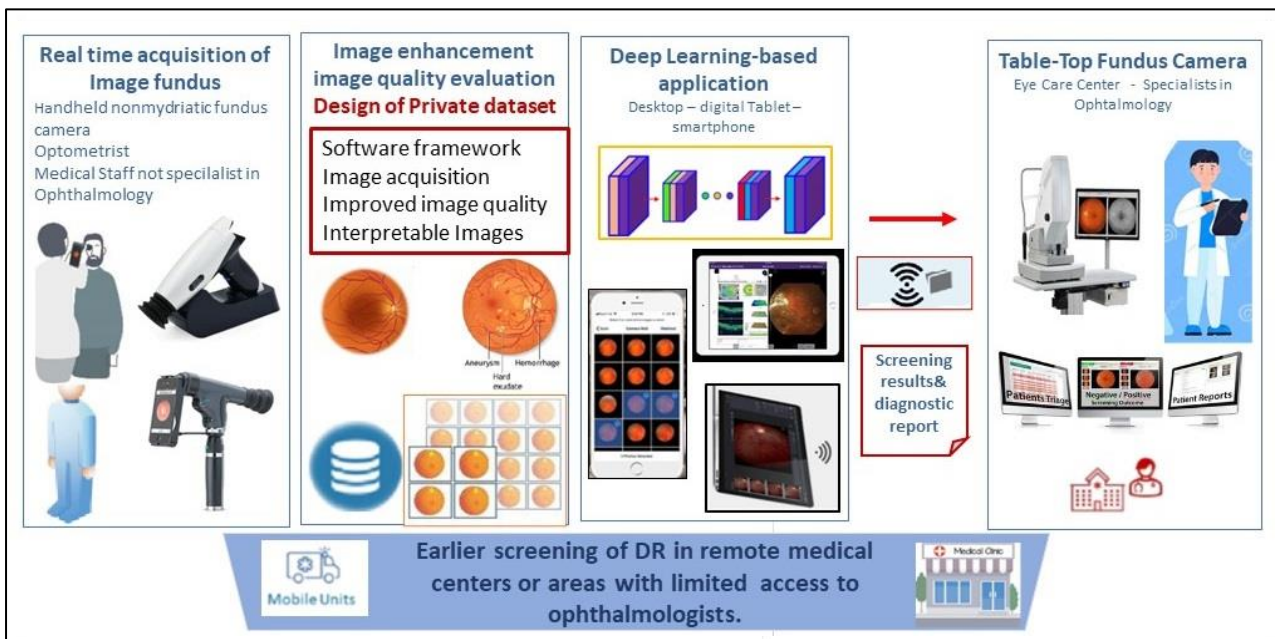


Fig. 1 : The Teleophthalmology Process of Our Innovative Approach providing itinerant visual care in rural areas connected to a pilot site

Our designed system will contribute towards providing the health-care solutions at the doorsteps of the patients; easing the workload of ophthalmologists and unavailability or shortage of expensive ophthalmology devices needed for visual exploration assessments. The accuracy of the diagnosis is dependent on both: quality of the acquired retinal images and robustness of the early diagnosis assistance application. The images acquired by portable retinal cameras may have limitations such as blurred or noisy images marred by specific

from the private database are acquired in real time by the oDocs nun IR portable camera, thereby making our study more applicable on real subjects.

3. We designed an automated software application capable of operating from a Desktop, which assists in early diagnosis of DR.

The rest of the paper is organized as follows. Section II reviews the existing efforts on earlier screening of DR from

retinal images using handheld portable non-mydratric fundus camera. Section III details our comparative study and analysis of fundus image enhancing methods. Section IV describes the development of deep transfer learning models for Early Diabetic Retinopathy Screening (i.e., Non-Proliferative Diabetic Retinopathy), including: the used datasets, data preparation & training, creating the DNN model for earlier DR screening, performance results & discussion, and software framework implementation as Desktop app. Finally, we conclude in Section V.

II. RELATED WORK

There are several levels of severity associated with the disease of DR. The main levels can be categorized in either non-proliferative (NPDR) or proliferative DR with Proliferative DR (PDR) being the advanced stage. NPDR is further categorized into three stages: mild, moderate, and severe [1]. For the purpose of DR detection, numerous computer-based techniques have been developed and reported in the literature. More recently, researchers have started using deep learning techniques for DR detection as deep learning algorithms - particularly transfer learning approach - have demonstrated promising results for image processing tasks.

The DR detection phases can be divided into two categories: binary classification, i.e., detecting the presence or absence of DR, and categorization into five stages. These types of image classification tasks can be grouped into conventional image processing techniques that use deep learning mechanisms such as deep convolutional neural networks (DCNNs) [4]. The diagnosis of ocular diseases frequently involves the use of a fundus camera, which has shown effective and efficient results when employed for screening retinal diseases such as DR [5]. The portability of a handheld fundus camera might render it an alternate tool for cost-effective DR screening. Additionally, it is also a suitable option for teleophthalmology consultations in cases when they are not readily accessible. Currently, digital tablets and smartphones are being utilized to collect the patient's ocular images, which might be shared with the ophthalmologist for further medical evaluation and diagnosis [6] [7]. Many computer-aided diagnosis methods for early screening, detection & grading of DR have been developed. Researchers have recently used deep learning models for DR detection, due to their success in image processing tasks. E.g., in [8] the authors have implemented a CNN using standard trainable and non-linear layers, for classification. Transfer learning techniques offer great advantages in achieving high performance while reducing training time, memory requirements, and network design efforts [9]. One of the contributions, of this work [9], is the overview of DL algorithms applications to classification-based studies in DR detection, by using fundus imaging. We focused on the efforts carried out between 2016 and 2021. We observed that most of the papers we surveyed were focused on the transfer learning DCNN models for DR detection and grading [10]. To address the challenging goal of earlier screening and detection of the ocular diseases like DR, the use of handled and portable fundus cameras has become crucial to the development of Tele-ophthalmology enhancing DR screening. In this study [11], the Optomed Aurora portable fundus camera outperformed the standard table-top fundus

camera, in terms of sensitivity and specificity for DR screening. In this work [12], three portable fundus cameras: iNview, Peek Retina and Pictor Plus, are compared for their sensitivity and specificity in detecting ocular diseases like DR. These fundus cameras demonstrated good results and effectively detected DR, when used for tele-ophthalmology retinal screening consultations. T.W. Rogers [13] uses a handheld portable fundus camera - Pictor Plus, Volk Optical Inc., USA - and performs DR grading using deep learning system, Pegasus (AI software, Visulytix Ltd., UK), which resulted in 89.4% and 94.3% detection rates, for RDR and PDR AUROC curves, respectively. The conducted study was a part of the Mexican Advanced Imaging Laboratory for Ocular Research (MAILOR) cohort.

The work presented in this article aims to deploy a telemedicine network for ocular diseases. Our ultimate objective is to design and develop a Desktop/smartphone based mobile platform, which employs sophisticated Deep Learning models and portable retinal cameras for screening and early diagnosis of ocular pathologies such as DR. In this endeavor, we are collaborating with the Ophthalmology Center and Vision Center at Omar Drissi Hospital, CHU HASAN II, Fez [14] [15]. Other than DR, our proposed approach has potential uses in other eye-related diseases, one can relate to our work on Glaucoma [16] and AMD (age-related macular degeneration) [17].

III. COMPARATIVE STUDY AND ANALYSIS OF FUNDUS IMAGE ENHANCEMENT TECHNIQUES

Retinal image fundus suffers a lot from contrast problems such as noise and intensity inhomogeneity (low-contrast, low-saturation). These various artefacts observed make up an impact on the quality of the images acquired particularly by handled and portable fundus camera. Retinal images preprocessing becomes a primary crucial step in the detection and classification of retinal diseases, such DR [5]. The application of enhancement techniques to retinal images proves invaluable in mitigating noise, enhancing brightness, and refining image contrast. By employing mathematical methods, it becomes feasible to augment the initial image quality and information content. This improvement confers significant advantages in recognizing distinctive features and facilitating subsequent image analysis, enabling ophthalmologists to achieve early detection of retinal pathologies, particularly RD. The comprehensive framework proposed for enhancing retinal images is visually illustrated in Figure 2.

This Framework has a few important steps to enhance retinal fundus images. To begin, we capture the retinal image, followed by resizing to optimize dimensions. Resizing is employed to decrease processing time. Subsequently, the image is divided into its distinct color components (red, green, blue). Focusing on the green channel is crucial because it harbors the most intricate details in the image's colors [5]. Afterward, image enhancement occurs by employing various filters. Additionally, combinations of smoothing and sharpening filters are applied in sequences to further refine the enhanced image. Finally, we evaluate the effectiveness of the process using metrics such as PSNR, SSIM, and RCEF. These metrics offer insights into the quality of the final image and gauge the performance of each step in the process.

A. Capture of Retinal fundus image by handled camera

The oDocs Nun IR retinal camera is a non-mydratric device with several key features that make it suitable for early detection of DR. It offers high-quality imaging capabilities with a resolution of 2880 x 2160 pixels, allowing for precise analysis of retinal images. The camera provides a wide field of view (FOV) ranging from 45 to 55 degrees, enabling a

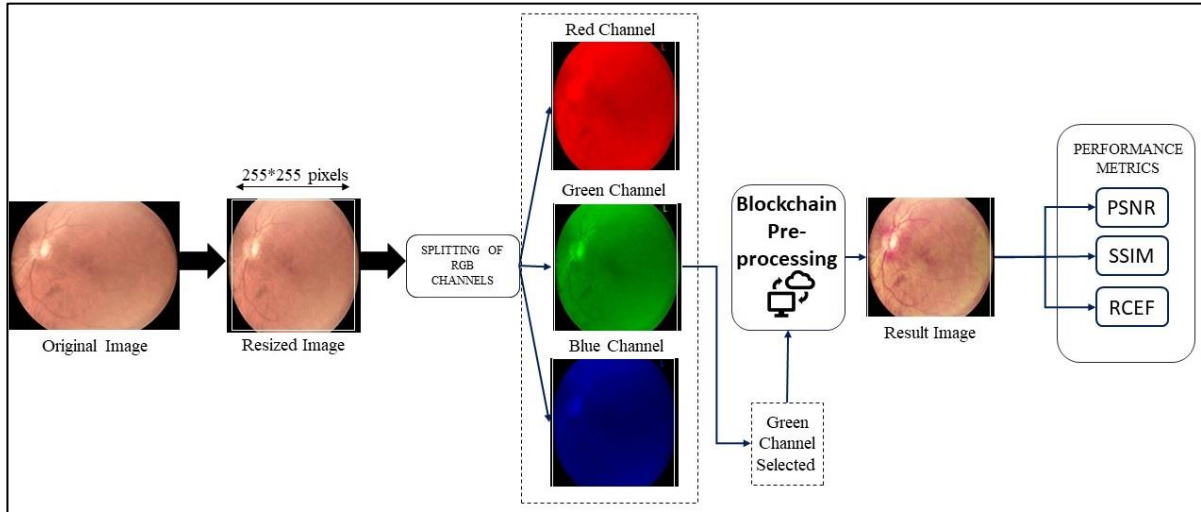


Fig. 2: Block diagram for retinal image enhancement.

panoramic view of the retina. It also includes a manual focusing function, allowing users to adjust the image sharpness within a range of -20D to +20D. The oDocs Nun IR camera is compatible with Android smartphones, providing flexibility and mobility in its usage.

The private dataset used for the early detection of DR was collected in collaboration with the Department of Ophthalmology at Omar Drissi Hospital (CHU HASAN II) in Fez, Morocco. The dataset consists of fundus images obtained using the oDocs Nun IR camera, specifically from individuals diagnosed with DR. It encompasses a wide spectrum of image qualities. Figure 3 presents a diverse selection of fundus images from our privately collected database, exhibiting notable high-quality attributes such as precise details, minimal noise, and enhanced contrast. These qualities contribute to a clear visualization of the retinal structures.

Conversely, the dataset also comprises images of lower quality, characterized by blurriness, noise, and inadequate contrast enhancement. Consequently, additional image processing techniques are required to ensure accurate analysis and interpretation.

B. Proposed flowchart of comparative study and analysis of enhancement techniques

Image quality improvement methods are used to make images better by reducing unwanted disturbances, making important parts more visible, and enhancing overall picture quality. One way to enhance image quality is by making differences between dark and light areas more noticeable. This can be done using tools called filters to be identified as a low image processing. There are many types of filters that can be used to make images look better, like ones that make the image softer, sharpen its details, or highlight its edges. This article presents eleven simple filters that can enhance the quality of retinal images, as indicated in article [18]. These

filters have proven to be reliable in improving the clarity of blood vessels in the images. Before applying these filters, the images undergo some initial preprocessing steps, such as resizing and focusing on the 'green' components. These green components contain the most detailed information regarding the image's colors. The introduced filters consist of the median filter (MF), the non-local means filter (NLM), the

Gaussian filter (GF), HE, contrast-limited histogram equalization (CLAHE), bottom hat filter (BHF), bilateral filter (BF). These filters are described with their respective mathematical formulas, and the resulting images they produce are illustrated in Table I.

In the context of the 11-filter array, let us explore the Median Filter and CLAHE as illustrative instances. The median filter is a noise reduction technique that preserves edges by replacing pixels with the median value of their neighbors. This is particularly useful for retinal images as it helps eliminate noise-induced extreme values. On the other hand, the CLAHE filter enhances contrast by adjusting pixel values according to local regions. This method is effective for highlighting important details like blood vessels, though its careful application is necessary to avoid noise amplification. Both filters contribute significantly to improving the quality and analyzability of retinal images.

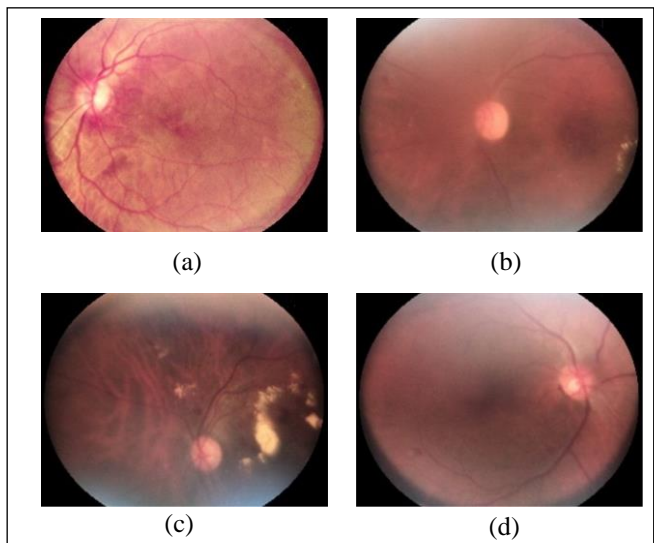
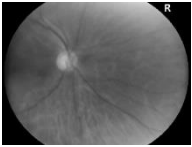

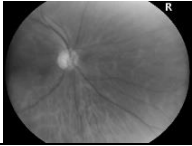
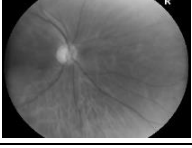
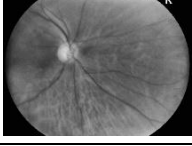


Fig. 3: Example of Image Clarity (a), Blurriness (b), Contrast (c), and Brightness Variation (d) from private dataset.

TABLE I. FILTERS WITH THEIR MATHEMATICAL EXPRESSIONS AND OUTPUT IMAGES

| Filters | Mathematical expressions | Output images |
|---------|---|---|
| MF | $\mathbf{g}(x, y) = \text{median}\{\mathbf{f}(n, m)\}$ |  |
| GF | $\mathbf{G}(x, y) = \frac{1}{2\pi\sigma^2} e^{-(x^2+y^2)/2\sigma}$ |  |
| BF | $\mathbf{I} = \frac{1}{w_p} \sum_{x_i} \mathbf{I}(x_i) \mathbf{f}_i(\ \mathbf{I}(x_i) - \mathbf{I}(x)\)$ |  |
| NLM | $\text{NLM}(x) = \left(\frac{1}{z(x)}\right) * \sum (w(x, y) * f(y))$ |  |
| CLAHE | $\mathbf{g} = [\mathbf{g}_{\max} - \mathbf{g}_{\min}] * \mathbf{p}(\mathbf{f}) + \mathbf{g}_{\min}$ |  |

We implemented and evaluated the enhanced median filter (IMF), as well as median filter combined with an average filter (MMF) [19]. It is observed that the MMF gives better results in terms of PSNR, SSIM, RCEF, which allows us to use it to improve image quality like other filters [20].

C. Image enhancement chains and image quality Evaluation

1) Enhancement chains:

The best improvement results obtained for the filters are chosen to build preprocessing chains. A chain comprising various stages: denoising, contrast enhancement and applying adaptive gamma correction. Among the more effective filters obtained: MF, GF, BF, NLM, and CLAHE. MF, GF, BF, and NLM function as smoothing filters, while CLAHE serves as the sharpening filter. This leads to a combination of smoothing and sharpening filters. Adaptive Gamma Correction is a technique that adjusts the intensity values of pixels in an image based on a gamma correction curve. According to this formula, for an 8-bit image of size $m \times n$ pixels, the gamma correction transforms the intensity value of the pixel at each spatial position (x, y) according to the following expression:

$$I_{gam}(x, y) = I(x, y)^\gamma \quad (1)$$

Where $I_{gam}(x, y)$ represents the gamma-corrected intensity of the image $I(x, y)$, and γ represents different gamma values that control the type of mapping. When γ is set to a value $\gamma > 1$, the dark regions of the original image become brighter in the gamma-corrected intensity image. Conversely, when γ is set to a value $\gamma < 1$, the bright regions of the original image become darker in the gamma-corrected intensity image [20]. It is important to note that the gamma value is adaptive for

each image, which means that each image has its own gamma value based on its intensity characteristics.

2) Performance metrics:

The performance of the image processing algorithms or enhancement filters can be evaluated by various quantitative measures. The metrics such as peak signal-to-noise ratio (PSNR), root mean square error (RMSE) and structural similarity index measure (SSIM) are used to find which image enhancement techniques give better results. PSNR is the most commonly used metric for image enhancement techniques and is given by:

$$PSNR = 10 \log_{10} \frac{255^2}{\frac{1}{MN} \sum_{ij} [g_{ij} - f_{ij}]^2} \text{ dB} \quad (2)$$

Where f and g are the original and the enhanced images and M and N are the row and column pixels in the image, respectively. The highest PSNR value gives better performance. The change in the structural similarity between the original and enhanced images is measured by SSIM and is given by:

$$SSIM(x, y) = \frac{(2\mu_x\mu_y + c_1)(2\sigma_{xy} + c_2)}{(\mu_x^2 + \mu_y^2 + c_2)(\sigma_x^2 + \sigma_y^2 + c_2)} \quad (3)$$

Where μ_x and μ_y are the average of x and y , respectively; σ_x^2 , σ_y^2 and σ_{xy} are the variance and covariance of x and y ; and c_1 and c_2 are variables. The values range from -1 to 1 ; if the value is exactly one it is considered to be of perfect structure similarity and if the value is lower, then there is no structural similarity. The dynamic range of histogram is measured using RCEF and is given by:

$$RCEF = \frac{\sigma_B^2 / \mu_B}{\sigma_A^2 / \mu_A} \quad (4)$$

Where σ_A and σ_B are the standard deviation of the original and enhanced image, and μ_A and μ_B are the mean of the original and enhanced image, respectively. For better enhancement, RCEF should be greater than 1.

3) Image quality Evaluation:

The table II of filter chains clearly shows that the PSNR value is high for GF + CLAHE+AGC, the SSIM value close to 1 for MMF + CLAHE+AGC and the RCEF value is better for NLM + CLAHE+AGC. These findings suggest that the selected best-performing combination could be a valuable asset in early detection for retinopathy (No RD, RD) cases. Figure 4 showcases the outcomes of the best optimal preprocessing blockchain, yielding the respective output images for (a) and (b), denoted as (a') and (b') in the sequence. The processing chain involves the application of a Gaussian Filter followed by merging channels. The Gaussian Filter helps in reducing noise and smoothing the images, while the merging channels operation combines the different color channels to create the final enhanced output. This procedure aims to enhance the quality of retinal images, enabling improved analysis and interpretation for various applications.

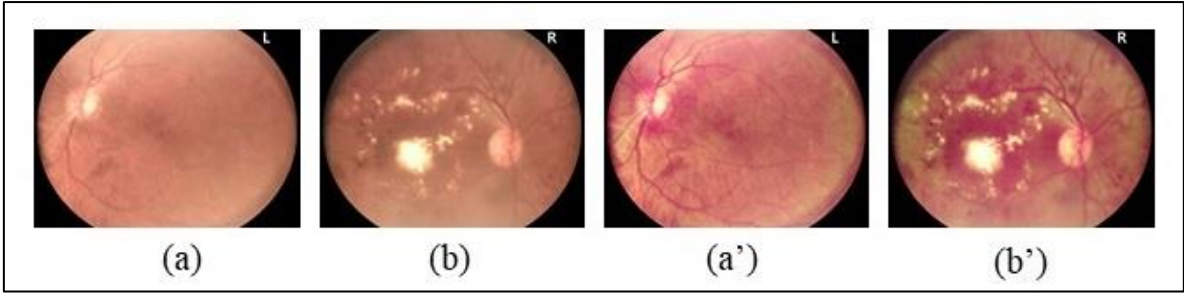


Fig. 4 : The best enhancement chain involves Gaussian Filter, CLAHE and Gamma correction to improve retinal image quality (a) and (b) original images, (a') and (b') are the output results corresponding to (a) and (b) respectively.

TABLE II. PERFORMANCE EVALUATION OF IMAGE QUALITY USING PSNR, SSIM, AND RCEF METRICS

| Blockchain | | SSIM | PSNR | RCEF |
|------------|---------------|--------|---------|---------|
| CH 1 | MF+CLAHE+ACG | 0,9804 | 33,2531 | 1,03774 |
| CH 2 | GF+CLAHE+ACG | 0,9803 | 33,2850 | 1,03767 |
| CH 3 | BF+CLAHE+ACG | 0,9803 | 33,2317 | 1,03783 |
| CH 4 | NLM+CLAHE+ACG | 0,9804 | 33,2096 | 1,03819 |
| CH 5 | MMF+CLAHE+ACG | 0,9804 | 33,2641 | 1,03768 |

IV. FINE-TUNING OF DEEP TRANSFER LEARNING MODELS FOR EARLIER SCREENING OF DIABETIC RETINOPATHY

Diabetic retinopathy (DR) is a prevalent ocular pathology observed in individuals with diabetes. It is a progressive complication that can lead to vision impairments and, in severe cases, total blindness. However, timely detection and appropriate treatment can potentially slow down or even arrest the progression of the disease. As a result, early screening for DR plays a crucial role in the effective management of diabetic patients. By identifying DR at its early stages, healthcare professionals can intervene promptly, implement suitable interventions, and optimize patient outcomes [21].

The early screening for DR involves two distinct stages: non-proliferative DR (NPDR) and proliferative DR (PDR). NPDR represents the initial stage of the disease, characterized by retinal lesions such as microaneurysms, haemorrhages, and exudates, as shown in (Fig5. b). Although these lesions might not immediately lead to significant vision loss, they serve as early indicators of the disease's presence. On the other hand, PDR corresponds the advanced stage, characterized by the formation of new abnormal blood vessels in the retina. These vessels are often fragile and can result in hemorrhages, retinal deformations, and deterioration of vision. The progression of PDR can be rapid, necessitating urgent medical intervention to avert permanent vision loss. Therefore, regular fundus examinations of the eye are essential for detecting both stages of diabetic retinopathy. During these inspections, an ophthalmologist assesses the retina using tools such as an ophthalmoscope or a retinal camera. The acquired images enable the visualization of characteristic DR lesions and facilitate the determination of the disease stage [22]. In this study, a combination of the three non-proliferative diabetic retinopathy (NPDR) stages (minime, moderate, severe) and the PDR into a single class named "DR" is considered, while keeping the "No DR" class separate. Figure 5 shows the

original images (a), (c) and (e) from the private database, APTOS and EyePACS respectively, and the corresponding results of the optimal preprocessing blocks (b), (d) and (f) used in this research.

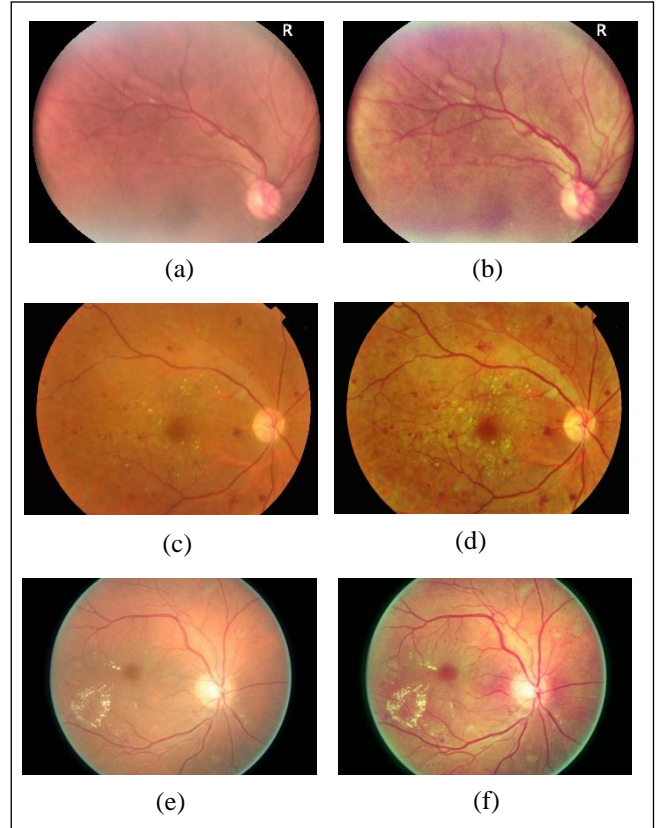


Fig. 5: Example images of dataset (a) and (b) private dataset, (c) and (d) APTOS dataset, (e) and (f) EyePACS dataset.

A. Datasets, data preparation and training

The growing requirement for model validation and training has prompted research groups to create their exclusive databases, now made accessible to the general public [23]. Particularly, the APTOS and EyePACS open-access dataset have garnered significant recognition for their availability of high-resolution fundus images. In contrast, a privately-owned dataset is employed to assess the effectiveness of developed diabetic retinopathy detection system.

1) Public Datasets

• APTOS

The APTOS 2019 Blindness Detection dataset proves to be a valuable resource for researchers and practitioners in the field of diabetic retinopathy (DR). This dataset encompasses a

collection of fundus images effectively portraying the five distinct stages of DR. Each image is thoroughly labelled with a severity level, which spans the spectrum from 0 to 4. These severity levels correspond to specific categories: label 0 signifies the absence of DR, label 1 indicates mild DR, label 2 represents moderate DR, label 3 denotes severe DR, and label 4 is indicative of proliferative DR. In total, the dataset consists of 3,662 retinal images. Among these, 1,805 images are meticulously classified as exhibiting no DR, 370 images labelled as mild DR, 999 images classified as moderate DR, 193 images identified as severe DR, and 295 embody the characteristics of proliferative DR. The fundus images' resolution within this dataset maintains a high standard at 3216×2136 pixels, ensuring a repository of visual with remarkable quality, optimally suited for analysis and evaluation endeavours [24].

- EyePACS

The EyePACS dataset, similar to the APTOS dataset, provides an extensive compilation of fundus images capturing the complete spectrum of DR progression across its five stages. Comprising a total of 35,126 retina images, with each image corresponding to both the left and right eyes. These images boast dimensions of 3888×2951 pixels, ensuring high-resolution visual data for analysis and research purposes. Within the EyePACS dataset, the images are meticulously categorized according to the five DR stages. Specifically, there are 25,810 images labeled as having 0 DR (no DR), 2,443 images classified as mild DR, 5,292 images portraying moderate DR, 873 images indicating severe DR, and 708 images showcasing proliferative DR. For the training process of the proposed model, a random selection strategy is adopted, choosing 1,534 images from the no DR stage and 2,764 images from the DR stage [27].

2) Private Dataset

The collected private dataset encompasses 1319 labelled images representing the five stages of diabetic retinopathy (DR), where a medical specialist undertook the task of assigning these labels. This dataset will serve as the foundation for this classification study, where the objective is devising a novel approach to accurately categorize the five stages of DR. It is worth noting that the medical specialist's labelling for each DR stage adhere to the established international standards. Within the dataset, there are 256 images denoting the absence of DR, 381 images with minimal non-proliferative diabetic retinopathy (NPDR), 335 images with moderate NPDR, 253 images capturing severe NPDR, and finally, 94 images showcasing proliferative diabetic retinopathy (PDR). The images were captured employing the oDocs nun IR device, renowned for its exceptional spatial resolution of 2880 x 2160 pixels accompanied by a field of view (FOV) ranging from 45 to 55 degrees.

3) Data Augmentation & Data splitting

In designed approach, a highly effective preprocessing pipeline was utilized, as detailed in the previous section, leading to promising outcomes. The pipeline involved resizing input images to dimensions of 224x224 pixels. Subsequently, a range of data augmentation techniques were applied to enrich the dataset. These techniques encompassed vertical and horizontal flipping, rotation at various angles, and adjustments to brightness and color settings. It is worth noting that the implementation of data augmentation considered a balanced factor for each stage to mitigate class

imbalance between the "NO DR" and "DR" classes. By incorporating these augmentation methods and maintaining balance across classes, the aim was to introduce heightened diversity and variability within the training data.

Table III outlines the distribution and number of images for each dataset, along with the count of images before and after data augmentation.

Several studies have employed various proportions to divide datasets into training, validation, and test sets. Furthermore, a common approach allocates 80% of the data for training, 10% for validation, and the remaining 10% for testing [25]. Alternatively, some studies have chosen to assign 75% of the data for training, with the remaining portion divided between validation and testing. In the specific case under consideration, a distribution of 75% for training, 15% for validation, and 10% for testing has been selected across all three datasets, based on the quantity of images in each dataset. The test set quantities for the privately-owned dataset, APTOS, and EyePACS are 720, 918, and 2000 images, respectively. The allocation of data into different subsets—namely, training, validation, and testing sets holds significant importance in optimizing the learning process and assessing model performance and generalization capabilities. In this context, the distribution of data emphasizes allocating a larger portion to the training set, which facilitates more effective learning by exposing the model to a diverse range of examples. This distribution strategy strikes a balance between maximizing the training data available to the model for effective learning and guaranteeing sufficient data for rigorous evaluation of performance and generalization potential.

TABLE III. DATASET DISTRIBUTION BEFORE AND AFTER DATA AUGMENTATION

| Dataset | Before data augmentation | | After data augmentation |
|---------|--------------------------|------------------|-------------------------|
| | Initial dataset | Dataset Selected | Dataset used |
| Private | 1321 | 1321 | 7200 |
| APTOS | 3662 | 2880 | 9566 |
| EyePACS | 35126 | 4290 | 20000 |

B. Designing DNN model for earlier screening of DR

In order to develop a deep neural network (DNN) model for the early detection of diabetic retinopathy, an approach employing transfer learning with three unique architectures is proposed (Fig. 6): DenseNet-121, Inception-v3, and MobileNetV2. The primary objective of this study is to accurately classify two stages of diabetic retinopathy: the presence or absence of DR. Through transfer learning with these three architectures, the extensive knowledge and insights gained from large-scale image datasets are leveraged. This approach substantially improves the ability to differentiate the initial phases of diabetic retinopathy, specifically the minimal and moderate DR stages, effectively leveraging the valuable information encapsulated within the pre-trained models.

The developed architectures undergo training for 200 epochs using the RMSProp optimization algorithm and the Binary Cross-Entropy (BCE) loss function. The learning rate is set to 0.001, and a fixed batch size of 64 is used for training and 32 for validation. To mitigate the risk of overfitting, the early stopping technique is incorporated, wherein training is halted after 50 epochs if there is no improvement in validation

accuracy. Furthermore, a dropout layer is introduced to the model to further address overfitting concerns. The validation accuracy is evaluated at each epoch, and the model with the highest validation accuracy is saved using the model checkpoint functionality of the Keras callback mechanism.

C. Performance results and discussion

- Implementation Framework

The outlined experimentation in this study was conducted on a computer system featuring an NVIDIA Corporation GP102GL [Quadro P6000]. The computer was equipped with an Intel (R) Xeon(R) Gold 6240R, 20 core with 2,40 GHz, and boasted a substantial RAM capacity of 377GB. The implementation of the models was performed using various software packages, including Python 3.10.9 and deep

$$\text{Accuracy} = \frac{TP + TN}{TP + FP + TN + FN} \quad (5)$$

$$\text{Sensitivity} = \frac{TP}{TP + FN} \quad (6)$$

$$\text{Specificity} = \frac{TN}{TN + FP} \quad (7)$$

$$\text{Precision} = \frac{TP}{TP + FP} \quad (8)$$

$$\text{F1 - Score} = 2 * \frac{\text{Precision} * \text{sensitivity}}{\text{Precision} + \text{sensitivity}} \quad (9)$$

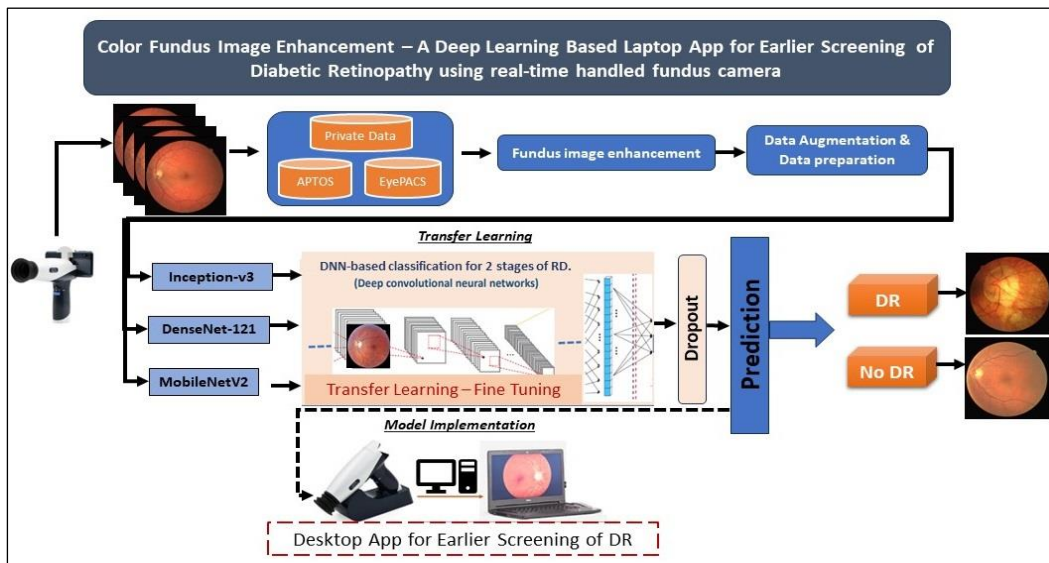


Fig. 6 : The flowchart of the proposed system DNN model for earlier screening of DR

learning libraries such as Keras with 3.10.9, Keras avec Tensorflow, OpenCV, Scikit-Learn were utilized in conjunction with the aforementioned libraries for the experimentations.

- Evaluation Metrics

Performance evaluations relies on five commonly used metrics, namely accuracy, sensitivity, specificity, precision, and F1-score, as shown in equations (5), (6), (7), (8), and (9), respectively. These metrics provide insights into different aspects of the classification model's performance.

Accuracy measures the proportion of correctly classified samples out of the total. It is calculated by dividing the sum of true positives and true negatives by the total number of samples. Sensitivity quantifies the proportion of actual positives correctly identified, while specificity assesses the proportion of actual negatives correctly identified. Precision evaluates the proportion of predicted positives that are truly positive. To provide a balanced measure considering both precision and sensitivity, the F1 score is used. The F1 score is calculated as the harmonic mean of precision and sensitivity, offering a comprehensive evaluation of the model's performance in identifying and predicting positive samples.

- Results and discussion

Fine-tuning involves adjusting the weights of a pre-trained model on a specific task using a smaller and task-specific

dataset. The idea is to take a model already trained on a general task and adapt it to the specific features of the desired early detection.

The classification results underwent testing using the collected private dataset and two public datasets, specifically APTOS and EyePACS, to evaluate the system's performance.

Table IV presents the better performance achieved by DenseNet-121 across the three datasets. With an accuracy of 98.6111%, sensitivity of 98.3333%, specificity of 100.0000%, precision of 98.8827%, and an F1-score of 70.0389%, DenseNet-121 demonstrates its superior predictive capabilities. Notably, on the APTOS and EyePACS datasets, it achieves accuracy of 97.3856% and 90.9000%, respectively. These results highlight the effectiveness of DenseNet-121 in accurately classifying diabetic retinopathy.

Table V summarizes the training and validation accuracy for each DNN architecture across the three databases. The findings clearly demonstrates that the DenseNet-121 model showcased improved classification performance, exhibiting superior results in both the training and validation stages. The assessment encompassed experimentation with the DenseNet-121, Inception-v3, and MobileNetV2 models to evaluate their performance. Among these models, DenseNet-121 consistently demonstrated superior predictive capabilities across all three datasets.

Furthermore, Figure 7 visually depicts the accuracy and loss during the training and validation stages of the diabetic retinopathy grading for the Private, APTOS, and EyePACS datasets. The consistent high accuracy and decreasing loss observed in the training and validation curves further validate the robustness and generalization capabilities of DenseNet-121.

TABLE IV. COMPARATIVE ANALYSIS OF PERFORMANCE METRICS FOR THREE ARCHITECTURES ON PRIVATE, APTOS, AND EYEPACS DATASETS

| Dataset | Test Prediction Evaluation Metrics | Architecture | | |
|---------|------------------------------------|-----------------|-------------|--------------|
| | | DenseNet-121 | MobileNetv2 | Inception-v3 |
| Private | Acc | 98.6111 | 96.1111 | 96.5278 |
| | Sen | 98.3333 | 94.7222 | 94.7222 |
| | Spe | 100.0000 | 99.7222 | 99.7222 |
| | Pre | 98.8827 | 97.4286 | 98.2709 |
| | F1-score | 70.0389 | 69.9029 | 66.9767 |
| APTOS | Acc | 97.3856 | 97.4946 | 98.0392 |
| | Sen | 97.0982 | 96.4286 | 97.7679 |
| | Spe | 100.0000 | 100.0000 | 99.7872 |
| | Pre | 97.5336 | 98.4055 | 98.2063 |
| | F1-score | 65.7856 | 70.2194 | 67.9818 |
| EyePACS | Acc | 90.9000 | 87.8500 | 89.1400 |
| | Sen | 93.9000 | 85.3000 | 88.1000 |
| | Spe | 99.4000 | 98.9000 | 98.9080 |
| | Pre | 88.5849 | 89.8841 | 89.8980 |
| | F1-score | 69.3722 | 70.0035 | 68.3761 |

TABLE V. TRAINING AND VALIDATION RESULTS COMPARISON OF THE THREE ARCHITECTURES

| Dataset | DenseNet-121 | | MobileNetv2 | | Inception-v3 | |
|---------|--------------|--------------|-------------|------------|--------------|------------|
| | Training | Validation | Training | Validation | Training | Validation |
| Private | 99.81 | 99.37 | 99.07 | 98.12 | 98.88 | 98.42 |
| APTOS | 98.91 | 98.81 | 98.68 | 98.51 | 98.61 | 98.61 |
| EyePACS | 94.06 | 93.92 | 94.54 | 92.16 | 91.30 | 91.43 |

The confusion matrix is a valuable tool that provides crucial insights into the performance of a model, enabling the evaluation of its accuracy in classifying instances of DR and No DR. The assessment of classification results for the DR and No DR categories was conducted across three distinct datasets using the confusion matrix. Figure 8 illustrates the confusion matrix for each dataset, highlighting the consistent superior performance of the DenseNet-121 architecture. Considering these findings, DenseNet-121 has been chosen as the preferred architecture due to its outstanding predictive capabilities.

D. Software Framework implementation as labtop app

The DenseNet-121 model, which has demonstrated superior performance in the performed evaluations, is implemented within a desktop application. This application is intended to function as a comprehensive tool for early diagnosis assistance of DR. The user interface, however, is developed using the programming language JavaScript. These frameworks have been chosen to enable the seamless integration of the DenseNet-121 model into the application, enabling efficient image processing and automatic DR diagnosis. Real-time image acquisition will be supported by the application, utilizing the oDocs nun IR camera connected to the Desktop. The camera is capable of capturing high-quality fundus images, allowing for accurate analysis and

diagnosis. Additionally, the incorporation of image enhancement techniques is planned to enhance the quality and clarity of the fundus images, ensuring optimal diagnostic accuracy.

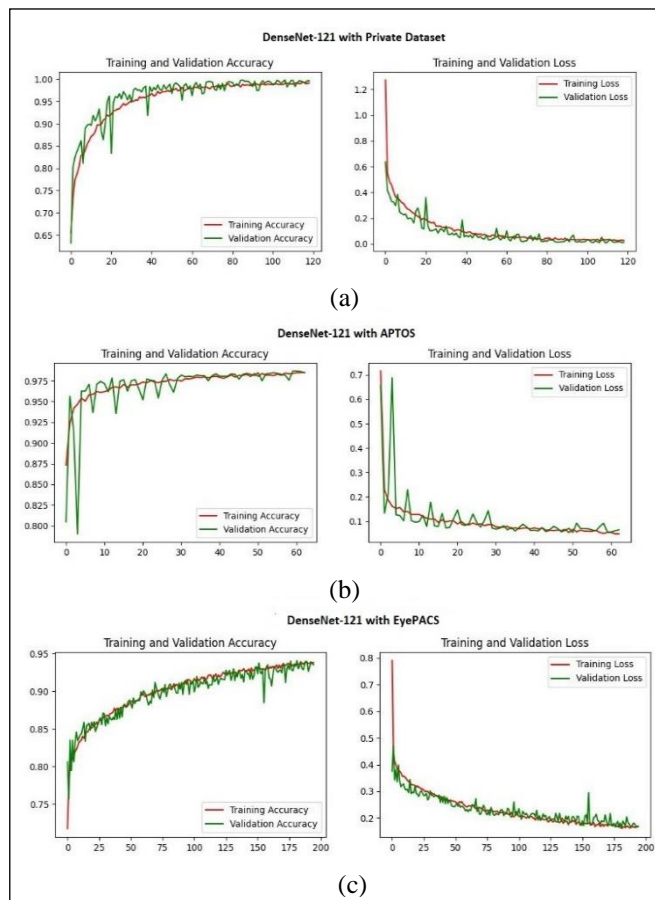


Fig. 7 : Accuracy and Loss in Training and validation for DenseNet-121 architecture on (a) private dataset (b) APTOS dataset and (c) EyePACS dataset

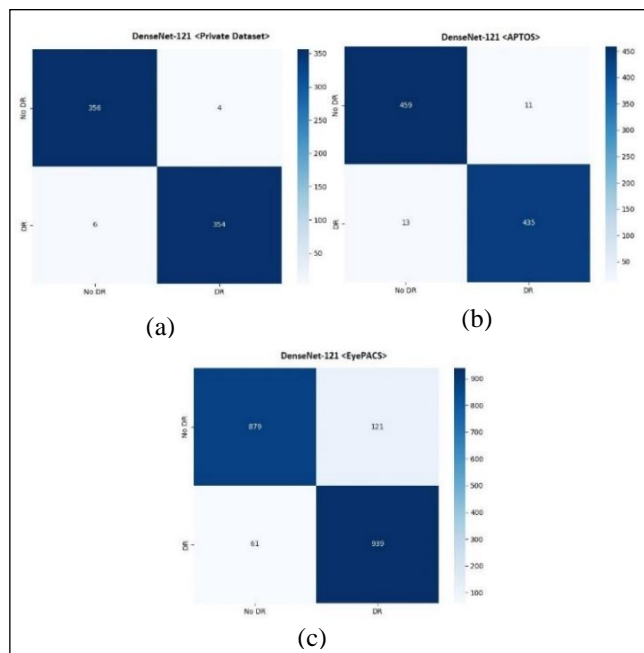


Fig. 8 : Confusion matrix of DenseNet-121 architecture on the (a) Private, (b) APTOS, and (c) EyePACS dataset

Furthermore, our vision extends beyond the diagnosis of DR alone. Once the system is established and validated for DR

detection, the system is generalized and expands its capabilities to detect other ocular pathologies such as glaucoma, age-related macular degeneration (AMD), and more. This will involve training the model on diverse datasets specific to each pathology, thus enabling clinicians to use the application as a versatile tool for multiple ocular conditions.

V. CONCLUSION

In this paper, we have developed a fine tuning and transfer learning-based deep convolutional neural network, for earlier screening of Diabetic Retinopathy. Our CNN is trained to effectively detect the DR at an earlier stage (Non-Proliferative Diabetic Retinopathy). The largest publicly available datasets of fundus images - APTOS and EyePACS datasets - were used to train and evaluate several transfer learning DCNN models. Our results show that the DenseNet-121 model generated the highest performance measures.

In this study, we built a private dataset from the image fundus of several patients, that were treated at the Eye Care Center of hospital Omar Drissi, CHU HASAN II, Fez, Morocco. The dataset is called the Diabetic Retinopathy Image Dataset and is used to detect DR in the image fundus, by employing the most effective DCNN model, DenseNet-121. A deep learning-based Desktop/smartphone app has been developed using a handled fundus camera. The developed app uses DCNN model (DenseNet-121) to classify the presence or absence of diabetic retinopathy (Non-Proliferative Diabetic Retinopathy, which is the early stage of DR), facilitating the earlier screening in remote medical facilities, or regions with limited access to resources such as ophthalmologists and Table-top fundus cameras.

ACKNOWLEDGMENT

We would like to express our sincere gratitude to the Gaspard Monge Computer Science Laboratory at ESIEE-Paris, Gustave Eiffel University, France, as well as the Ministry of Higher Education of Morocco for their support of the bilateral program, and to SIMAD-PR, N° 48672RG.

REFERENCES

- [1] M. J. Burton *et al.*, « The Lancet Global Health Commission on Global Eye Health: vision beyond 2020 », *Lancet Glob. Health*, vol. 9, n° 4, p. e489-e551, avr. 2021, doi: 10.1016/S2214-109X(20)30488-5.
- [2] G. Labiris, E.-K. Panagiotopoulou, et V. P. Kozobolis, « A systematic review of teleophthalmological studies in Europe », *Int. J. Ophthalmol.*, vol. 11, n° 2, p. 314-325, févr. 2018, doi: 10.18240/ij.o.2018.02.22.
- [3] « SMO – Société Marocaine d’Ophtalmologie (SMO) ». <https://smo.ma/>.
- [4] G. Quellec *et al.*, « Automatic detection of referral patients due to retinal pathologies through data mining », *Med. Image Anal.*, vol. 29, p. 47-64, avr. 2016, doi: 10.1016/j.media.2015.12.006.
- [5] S. Iqbal, T. M. Khan, K. Naveed, S. S. Naqvi, et S. J. Nawaz, « Recent trends and advances in fundus image analysis: A review », *Comput. Biol. Med.*, vol. 151, p. 106277, déc. 2022, doi: 10.1016/j.compbiomed.2022.106277.
- [6] M. E. Ryan *et al.*, « Comparison Among Methods of Retinopathy Assessment (CAMRA) Study », *Ophthalmology*, vol. 122, n° 10, p. 2038-2043, oct. 2015, doi: 10.1016/j.ophtha.2015.06.011.
- [7] R. Rajalakshmi *et al.*, « Validation of Smartphone Based Retinal Photography for Diabetic Retinopathy Screening », *PLoS ONE*, vol. 10, n° 9, p. e0138285, sept. 2015, doi: 10.1371/journal.pone.0138285.
- [8] V. Gulshan *et al.*, « Development and Validation of a Deep Learning Algorithm for Detection of Diabetic Retinopathy in Retinal Fundus

- Photographs », *JAMA*, vol. 316, n° 22, p. 2402-2410, déc. 2016, doi: 10.1001/jama.2016.17216.
- [9] N. Abou Baker, N. Zengeler, et U. Handmann, « A Transfer Learning Evaluation of Deep Neural Networks for Image Classification », *Mach. Learn. Knowl. Extr.*, vol. 4, p. 22-41, janv. 2022, doi: 10.3390/make4010002.
- [10] N. Tsiknakis *et al.*, « Deep learning for diabetic retinopathy detection and classification based on fundus images: A review », *Comput. Biol. Med.*, vol. 135, p. 104599, août 2021, doi: 10.1016/j.compbiomed.2021.104599.
- [11] E. Midena *et al.*, « Handheld Fundus Camera for Diabetic Retinopathy Screening: A Comparison Study with Table-Top Fundus Camera in Real-Life Setting », *J. Clin. Med.*, vol. 11, n° 9, p. 2352, avr. 2022, doi: 10.3390/jcm11092352.
- [12] L. Lu *et al.*, « Diagnostic accuracy of handheld fundus photography: A comparative study of three commercially available cameras », *PLOS Digit. Health*, vol. 1, n° 11, p. e0000131, nov. 2022, doi: 10.1371/journal.pdig.0000131.
- [13] T. W. Rogers *et al.*, « Evaluation of an AI system for the detection of diabetic retinopathy from images captured with a handheld portable fundus camera: the MAILOR AI study », *Eye*, vol. 35, n° 2, Art. n° 2, févr. 2021, doi: 10.1038/s41433-020-0927-8.
- [14] C. Khodris, B. Ahmed, C. Fouad, A. Meriem, B. A. Idriss, et H. Tairi, « Artificial intelligence in ophthalmology: the ophthalmologist’s opinion », in *2020 International Conference on Intelligent Systems and Computer Vision (ISCV)*, Fez, Morocco: IEEE, juin 2020, p. 1-5. doi: 10.1109/ISCV49265.2020.9204195.
- [15] M. Hassan, B. Ahmed, C. Fouad, A. Meriem, A. Benatiya, et B. M. Faouzi, « Ganglion Cell Layer Analysis in Nonarteritic Anterior Ischemic Optic Neuropathy in Diabetic Patients: From the Acute to Resolving Phases », *J. Res. Med. Dent. Sci.*, vol. 9, n° 11, 2021.
- [16] A. Mvoulana, R. Kachouri, et M. Akil, « Fully automated method for glaucoma screening using robust optic nerve head detection and unsupervised segmentation based cup-to-disc ratio computation in retinal fundus images », *Comput. Med. Imaging Graph.*, vol. 77, p. 101643, oct. 2019, doi: 10.1016/j.compmedimag.2019.101643.
- [17] S. B. Sayadia, Y. Elloumi, R. Kachouri, M. Akil, A. B. Abdallah, et M. H. Bedoui, « Automated method for real-time AMD screening of fundus images dedicated for mobile devices », *Med. Biol. Eng. Comput.*, vol. 60, n° 5, p. 1449-1479, mai 2022, doi: 10.1007/s11517-022-02546-8.
- [18] E. Erwin, « Improving Retinal Image Quality Using the Contrast Stretching, Histogram Equalization, and CLAHE Methods with Median Filters », *Int. J. Image Graph. Signal Process.*, vol. 12, p. 30-41, avr. 2020, doi: 10.5815/ijgisp.2020.02.04.
- [19] « Median Filtering - Computer Vision Website Header ». https://www.southampton.ac.uk/~msn/book/new_demo/median/.
- [20] S. Dash et M. R. Senapati, « Enhancing detection of retinal blood vessels by combined approach of DWT, Tyler Coye and Gamma correction », *Biomed. Signal Process. Control*, vol. 57, p. 101740, mars 2020, doi: 10.1016/j.bspc.2019.101740.
- [21] W. Zhang *et al.*, « Automated identification and grading system of diabetic retinopathy using deep neural networks », *Knowl.-Based Syst.*, vol. 175, p. 12-25, juill. 2019, doi: 10.1016/j.knosys.2019.03.016.
- [22] S. Ramchandre, B. Patil, S. Pharande, K. Javali, et H. Pande, « A Deep Learning Approach for Diabetic Retinopathy detection using Transfer Learning », in *2020 IEEE International Conference for Innovation in Technology (INOCON)*, nov. 2020, p. 1-5. doi: 10.1109/INOCON50539.2020.9298201.
- [23] K. C. Jordan, M. Menolotto, N. M. Bolster, I. A. Livingstone, et M. E. Giardini, « A review of feature-based retinal image analysis », *Expert Rev. Ophthalmol.*, vol. 12, n° 3, p. 207-220, mai 2017, doi: 10.1080/17469899.2017.1307105.
- [24] C. Mohanty *et al.*, « Using Deep Learning Architectures for Detection and Classification of Diabetic Retinopathy », *Sensors*, vol. 23, n° 12, p. 5726, juin 2023, doi: 10.3390/s23125726.
- [25] K. Xu, D. Feng, et H. Mi, « Deep Convolutional Neural Network-Based Early Automated Detection of Diabetic Retinopathy Using Fundus Image », *Molecules*, vol. 22, n° 12, Art. n° 12, déc. 2017, doi: 10.3390/molecules22122054.
- [26] M. S. Patil, S. Chickerur, C. Abhimalya, A. Naik, N. Kumari, et S. Maurya, « Effective Deep Learning Data Augmentation Techniques for Diabetic Retinopathy Classification », *Procedia Comput. Sci.*, vol. 218, p. 1156-1165, 2023, doi: 10.1016/j.procs.2023.01.094.
- [27] N. Band *et al.*, « Benchmarking Bayesian Deep Learning on Diabetic Retinopathy Detection Tasks ». arXiv, 23 novembre 2022.